Electronic structure of YMn_2 and $Y_{0.96}Lu_{0.04}Mn_2$ studied by x-ray emission spectroscopy

Hitoshi Yamaoka,[1] Naohito Tsujii,[2] Ignace Jarrige,[3] Yoshinori Takahashi,[4] Jesús Chaboy,[5] Hirofumi Oohashi,[6] Katsumi Handa,[7] Junko Ide,[7] Tatsunori Tochio,[8] Yoshiaki Ito,[7] Tomoya Uruga,[9] and Hideki Yoshikawa[6]

[1]*Harima Institute, The Institute of Physical and Chemical Research (RIKEN), Sayo, Hyogo 679-5148, Japan*

[2]*Quantum Beam Center, National Institute for Materials Science, 1-2-1 Sengen, Tsukuba 305-0047, Japan*

[3]*Synchrotron Radiation Research Unit, Japan Atomic Energy Agency, 1-1-1 Kouto, Sayo, Hyogo 679-5148, Japan*

[4]*University of Hyogo, 3-2-1 Kouto, Kamigori, Ako, Hyogo 678-1297, Japan*

[5]*Instituto de Ciencia de Materiales de Aragón and Departamento de Física de la Materia Condensada, CSIC-Universidad de Zaragoza, 50009 Zaragoza, Spain*

[6]*Harima Office, National Institute for Materials Science, Sayo, Hyogo 679-5148, Japan*

[7]*Institute for Chemical Research, Kyoto University, Uji, Kyoto 611-0011, Japan*

[8]*Department of Physics, Kobe University, Kobe 657-8501, Japan*

[9]*Japan Synchrotron Research Institute, Sayo, Hyogo 679-5148, Japan*

(Received 30 April 2009; revised manuscript received 23 June 2009; published 9 September 2009)

Bulk electronic properties of Mn in the frustrated spin-fluctuation systems YMn_2 and $Y_{0.96}Lu_{0.04}Mn_2$ have been investigated using Mn K x-ray absorption spectroscopy in the partial fluorescence yield (PFY-XAS), Mn $K\beta$ x-ray emission (XES) and Mn $1s2p$ resonant x-ray emission spectroscopy (RXES). Based on both the PFY-XAS and RXES data, we observe a weakening (increase) of the density of states near the Fermi level in YMn_2 ($Y_{0.96}Lu_{0.04}Mn_2$) at low temperature, reflecting the changes in hybridization accompanying the unit-cell volume expansion (contraction). No valence mixing is observed in YMn_2. From the $K\beta$ emission spectra, Mn is found to retain its high-spin state upon temperature variation (18–311 K) and Lu substitution.

DOI: 10.1103/PhysRevB.80.115110 PACS number(s): 71.20.Eh, 75.25.+z, 75.50.Ee, 75.30.Mb

Laves phase compounds have the composition RMn_2 (R =rare earth) and they crystallize either in the C15 (cubic laves $MgCu_2$ type) or the C14 (hexagonal laves) structure. Among them, YMn_2 is well known as a three-dimensional frustrated itinerant electron antiferromagnet with spin fluctuations of large amplitude.[1] YMn_2 has the fcc-based C15 cubic structure with space group $Fd\bar{3}$ (O_h^7) (Ref. 2) and the Néel temperature is $T_N \approx 100$ K. Above T_N a large specific heat coefficient (γ) of 14 mJ/K^2 mol was reported.[3] At $T=T_N$ the volume increases discontinuously by 5% accompanying the antiferromagnetic (AF) order with a magnetic moment of $2.7\mu_B$ per Mn atom. A helical magnetic order was found by Ballou *et al.*[4] while Nakamura *et al.* proposed a model with double-axial spin structure.[5] Spin fluctuation was directly observed by neutron inelastic scattering.[4,6–10] The Mn magnetic moment in RMn_2 compounds is known to be very sensitive to the interatomic distance, below a critical value of which it is suppressed.[1,11,12] Shiga *et al.* suggested the magnetovolume effect as the origin of the transition from paramagnetic to AF phase.[1]

In YMn_2 a small substitution of Mn by Al,[13,14] Ni,[15,16] or Y by Sc,[14,17] Ce,[18,19] La,[17] Gd,[20] Tb,[5] and Lu,[21,22] has a drastic influence on the local magnetic moment through changes in the unit-cell volume. For instance, a 3% substitution of Sc to the Y site inhibits the magnetic order and results in an enormous specific heat coefficient (80 mJ/K^2 mol).[1] A similar effect was reported to occur under external pressure.[23–25] In these nonmagnetic samples the lattice constant monotonically decreases with temperature. Like a lot of heavy fermion compounds, the T^2 coefficient in the temperature dependence of the resistivity (A) and the T-linear specific heat coefficient (γ) of $Y_{0.97}Sc_{0.03}Mn_2$, with the ratio $A/\gamma \sim 10^5$ $\mu\Omega$ cm $(Kmol/mJ)^2$, fall on the Kadowaki-Woods plot.[26,27] Accordingly the Sc-substituted system, as well as YMn_2 above T_N, are taken as quantum spin liquids due to the geometrical frustration.

Theoretically, band calculations by Terao and Shimizu showed that an increase in the kinetic energy of the d electrons after the striction is compensated by the large value of the spontaneous volume magnetostriction.[28] A tight-binding Hubbard model calculation by Yamada *et al.* showed that the density of states (DOS) of YMn_2 near the Fermi edge (E_F) mainly consist of Mn d electrons.[29] Asano and Ishida argued that antiferromagnetism occurs because the Fermi level coincides with a dip in the DOS.[30] Kübler *et al.* performed density functional calculation for the AF state of YMn_2.[31] They showed that the total energy of the [000] AF state modulated by a long-period spiral is lower than the [001] state, at odds with neutron diffraction data that pointed to a [001] AF order.[32] Very recently, first principle calculations by Iwasaki *et al.* led to converging results with Kübler *et al.*[33]

Because the Fermi level of YMn_2 lies near a minimum in the DOS,[30,34] small changes in the DOS near E_F can easily induce modifications in the magnetic character. Despite the high relevance of the electronic structure to understand both magnetic and structural properties of this system, so far only photoelectron spectroscopy (PES) was applied to YMn_2 and $Y_{0.97}Sc_{0.03}Mn_2$.[35] The spectra in this study had a surface contribution as high as 30%. A weak narrowing of the DOS near E_F of $Y_{0.97}Sc_{0.03}Mn_2$ compared with YMn_2 was observed at low temperature. We here focus on the bulk electronic properties of Mn in YMn_2 and $Y_{0.96}Lu_{0.04}Mn_2$ and their temperature dependence. We employ Mn K x-ray absorption spectroscopy in the partial fluorescence yield mode (PFY-XAS), Mn $K\beta$ x-ray emission spectroscopy (XES) and Mn $1s2p$ resonant XES.[36–40] Our results provide new insight into the temperature dependence of the d DOS near E_F for these two

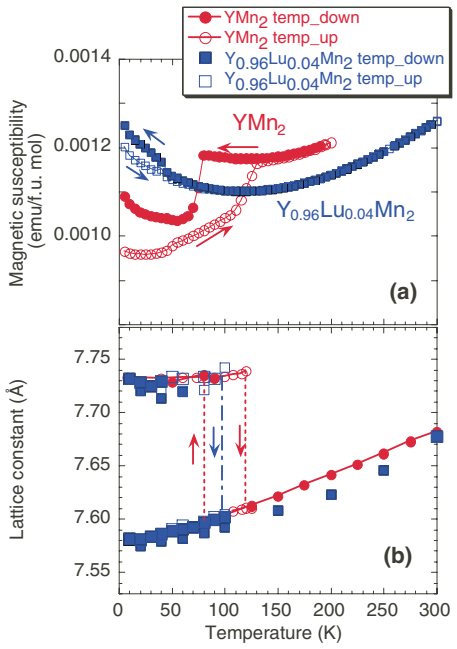

FIG. 1. (Color online) (a) Magnetic susceptibility of YMn_2 (closed circle: decreasing the temperature, open circle: increasing the temperature) and $Y_{0.96}Lu_{0.04}Mn_2$ (closed square: decreasing the temperature, open square: increasing the temperature) as a function of temperature. (b) Temperature dependence of the lattice constant.

systems, which we discuss based on the temperature dependence of the magnetic susceptibility and of the lattice constant. The Mn spin state is found to be independent of either temperature changes or Lu substitution. The Mn 3*d* states in YMn_2 are found relatively more delocalized at low temperature compared with 300 K. Strong 3*d*-4*p* hybridization is observed in both the paramagnetic and AF states of YMn_2.

Polycrystalline samples of YMn_2 and $Y_{0.96}Lu_{0.04}Mn_2$ were prepared by argon arc melting of pure metals and annealing in evacuated silica tubes. The Lu-substituted system has a large specific heat coefficient $\gamma=120$ mJ/K^2 mol (Ref. 22) and agrees well with the Kadowaki-Woods relation.[26,27] The results of the magnetic susceptibility (χ) measurement as a function of temperature are shown in Fig. 1(a). The temperature dependence of χ of YMn_2 shows a discontinuous change around 100 K, while for $Y_{0.96}Lu_{0.04}Mn_2$ the transition temperature is shifted down to 40 K and the hysteresis is much smaller compared with YMn_2. Figure 1(b) shows the temperature dependence of the lattice constant as estimated by x-ray diffraction, which roughly follows the change in the magnetic susceptibility. We observe that both paramagnetic and AF states coexist at low temperature in $Y_{0.96}Lu_{0.04}Mn_2$, suggesting that 4% is close to a critical value for the Lu substitution. This is consistent with the temperature dependence of the lattice parameter measured by Gaĭdukova *et al.*, according to which the critical value of Lu substitution is between 3% and 5%.[21]

X-ray spectroscopy measurements were carried out at the BL15XU undulator beamline in SPring-8.[41] The beam was monochromatized by a water-cooled double crystal monochromator with the resolution of about $E/\delta E \approx 10^4$ around 8 keV, where E is the photon energy. The signal emitted from

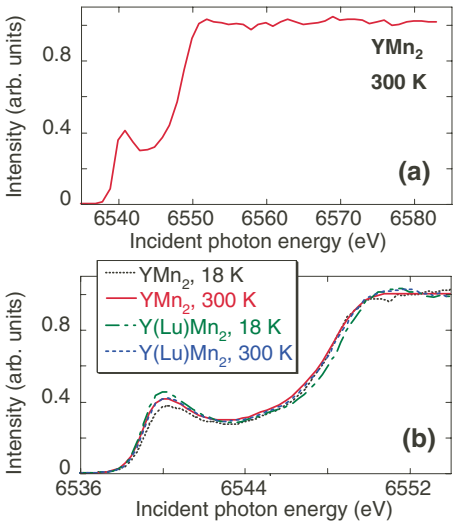

FIG. 2. (Color online) PFY-XAS spectra obtained for (a) YMn_2 at 300 K (solid line) and (b) YMn_2 (dotted line) and $Y_{0.96}Lu_{0.04}Mn_2$ at 18 K (long-dashed-dotted line) and 300 K (dashed line).

the sample was measured by a Ge 111 double crystal spectrometer with (+,+) geometry.[42] The total energy resolution of the spectrometer was about $E/\delta E \approx 3350$ at 8 keV. The reproducibility of the emission energy remained within ± 0.03 eV. Owing to the setup stability the energy position of the peaks could be determined within an order of magnitude better accuracy than the energy step.[40] An Iwatani CRT-M310-OP cryostat was used to cool the samples down to 18 K.

Figure 2 shows the Mn *K* PFY-XAS spectra obtained for both YMn_2 and $Y_{0.96}Lu_{0.04}Mn_2$ at 18 and 300 K. The spectra are normalized to their intensity at 6552.5 eV. We made self-absorption correction for the PFY-XAS spectra by using the computing code, Athena. The strong pre-edge feature centered around 6540 eV arises from transitions of 1*s* electrons promoted into the hybridized 3*d*-4*p* conduction states just above E_F.[16,19] The spectrum in the pre-edge region therefore reflects the presence of the empty Mn 3*d* DOS to the creation of a 1*s* core hole. The intensity of the pre-edge peak is clearly stronger than in Mn oxide compounds,[43] thus pointing to a strong *p*-*d* hybridization in YMn_2 and $Y_{0.96}Lu_{0.04}Mn_2$. We fitted the PFY-XAS spectra using a symmetric peak (Voigt) function for the pre-edge structure and two arctanlike functions (asymmetric double sigmoidal function) for the dipolar main edge. Actually the shape of the main-edge component is similar to the fluorescence component as will be shown in Fig. 6. The residual spectra after subtraction of the main-edge component are shown in Fig. 3(b), and the spectra normalized to the intensity of the peak are shown in Fig. 3(c) with an inset of enlarged figure.

Chaboy *et al.* interpreted the variations of near-edge line shape in terms of changes in the width and intensity of the DOS near E_F and shift of the Fermi edge.[19] Accordingly, the shoulderlike feature appearing at the threshold is due to the overlapping of the Mn empty *p* states with the outer *s*- and *d*-symmetry orbitals.[44] Therefore, the modification of the width and the intensity of the double-step near-edge structure is a fingerprint of hybridization changes of the outermost

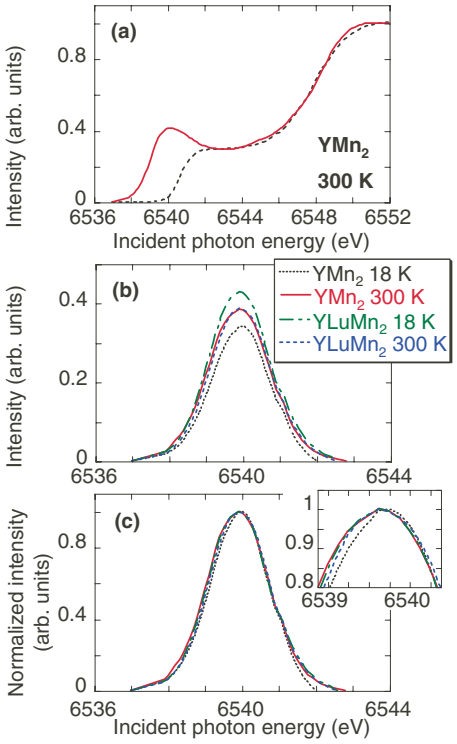

FIG. 3. (Color online) (a) Example of fit of the onset of the dipolar transitions (solid line) of the PFY-XAS spectrum (dotted line) of YMn_2 at 18 K. (b) Pre-edge features obtained from the data in Fig. 2(b) by subtracting the dipolar background. (c) Normalized pre-edge features to the maximum. The inset in (c) shows an expanded view of the maxima.

orbitals between the absorbing atom and the nearest neighbors.[45,46] We discuss our data along the same lines, starting with YMn_2. The onset of the AF order at low temperature in YMn_2 is accompanied by a volume increase.[47] Our results show a decrease in intensity of the pre-edge peak of YMn_2 at 18 K as seen in Fig. 3(b), pointing to a decrease of the Mn 3*d* DOS. This agrees well with the PES measurement in Ref. 35 which showed a small decrease of the DOS of YMn_2 in the vicinity of E_F at low temperature. We note that there is consistency as well with band calculations of YMn_2 and its hydrides,[48] where a decrease in the Mn *d* DOS near E_F was reported for the hydrides which have an expanded crystal lattice compared to YMn_2. This trend, though, is at odds with Ref. 1 where an increase of the interatomic distance was suggested to result in band narrowing and accordingly in an increase of the *d* DOS near E_F. Although correct, this reasoning does not account for the *d*-*d* hybridization decrease which is expected to accompany a unit-cell expansion, thus contributing to a reduction of the DOS at the Fermi level. It should be noted that as both Y and Lu are characterized by a large density of empty 5*d* and 4*d* states, respectively, the *d*-*d* hybridization refers to that of the absorbing Mn atom and its next neighbors, both Mn and Y(Lu) atoms, all of them contributing to the *d* states of the conduction band. We understand therefore that the volume dependence of the DOS is governed by two coexisting effects, and based on our data, we can conclude that the effect related to hybridization is dominant for YMn_2.

We now compare the YMn_2 and $Y_{0.96}Lu_{0.04}Mn_2$ spectra. Lu substitution to the Y site is expected to induce a contraction of the unit-cell volume because of the smaller atomic radius of Lu. Nonetheless, the difference between the lattice constant of YMn_2 and $Y_{0.96}Lu_{0.04}Mn_2$ at room temperature is very small as seen in Fig. 1(b). This explains the absence of dependence of the pre-edge region of the PFY-XAS spectrum on Lu substitution at 300 K as seen in Figs. 2(b) and 3(b). Turning now to the temperature dependence, the pre-edge peak of the Lu-substituted system is found to increase against the nonsubstituted one at 18 K [cf. Fig. 3(b)]. This is reminiscent of the slight increase reported in the PES spectrum near E_F for the Sc-substituted compound $Y_{0.97}Sc_{0.03}Mn_2$ compared with YMn_2 at 16 K.[35] An increase of the pre-edge peak of the Lu-substituted system at low temperature seems contradictory with the onset of the AF order and the associated volume expansion. But as seen in Fig. 1(b), in the low-temperature phase of $Y_{0.96}Lu_{0.04}Mn_2$, the paramagnetic phase, which follows a continuous thermal-contraction behavior, coexists with the AF phase. As discussed for YMn_2 above, contraction implies growth of *d*-*d* hybridization, resulting in an increase of the Mn *d* DOS near E_F. Therefore, the opposite temperature dependence of the pre-edge intensity of YMn_2 and $Y_{0.96}Lu_{0.04}Mn_2$ is well accounted for in terms of volume-induced changes in the hybridization; the expansion-induced DOS narrowing is not here the dominant effect.

We examine now the substitution dependence of the Fermi level. A shift in the Fermi level usually goes hand in hand with a change in the electron count. For instance, in the Ni-substituted case, a strong electronic perturbation of the Mn atoms resulting in an electron count variation is regarded as the origin of the Fermi level shift toward higher energies.[16] On the other hand, in the Ce-substituted material, a shift of +0.2 eV in the Fermi level was observed without any change in the electron count.[19] In this particular case, the shift was attributed to a strong localization-delocalization process inherent to the peculiar nature of the Ce electronic state. Neither such process, nor an electron count change, is to be expected for the Lu-substituted system. This likely explains the lack of clear substitution or temperature dependence of the Fermi level in our case as seen in Fig. 3(c).

Figure 4 shows Mn *K* $1s2p$ RXES spectra measured for YMn_2 at (a) 300 K and (b) 18 K for several values of the incident photon energy across the Mn *K* absorption edge, along with the Mn *K* PFY-XAS spectrum. The transfer energy is defined as the difference between the incident and emitted photon energies. We observe the Raman component at constant transfer energy around the pre-edge peak, while the growing fluorescence signal shifts toward high transfer energies as the incident energy is increased above the pre-edge peak [see Fig. 5(b)].[49] These two components were separated based on the fitting procedure detailed in Refs. 50 and 51. An example of fit is shown in Fig. 5(a) for an incident photon energy of 6539 eV. We used four symmetric functions in the fitting due to the asymmetric profile of the spectra, as performed in Cu metal.[39,52] Fig. 5(b) shows the relation of energy dispersion for the Raman and fluorescence components. Figure 6 shows the respective intensities of the Raman and fluorescence signals derived from the fitting, to-

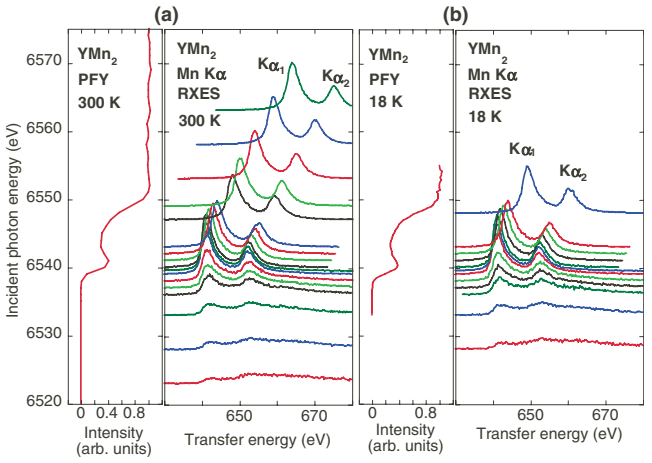

FIG. 4. (Color online) Mn K $1s2p$ RXES spectra obtained for YMn_2 at (a) 300 K and (b) 18 K for several photon energies across the Mn-K edge (right panel), along with the Mn K PFY-XAS spectrum (left panel). The vertical position of the RXES spectra is scaled to the E_{in} axis of the corresponding PFY-XAS spectrum.

gether with the PFY-XAS spectrum. The Raman component at 18 K seems to be slightly weaker and broader than at 300 K, concurring with the PFY-XAS results and seemingly reflecting the decrease of the DOS near the Fermi edge at low temperature. Interestingly, the Raman component is limited to the pre-edge region at both temperatures, 18 and 300 K, pointing to relatively delocalized Mn $3d$ states[53] independently of the magnetic order. Only one Raman component was sufficient for the curve fit, hence no valence mixing should occur for Mn in YMn_2.

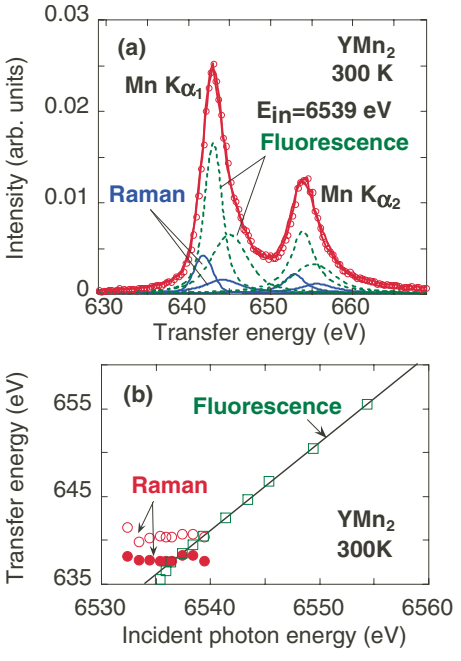

FIG. 5. (Color online) (a) Example of curve fit obtained for the Mn K $1s2p$ RXES spectrum measured on YMn_2 at 300 K and E_{in} =6539 eV (open circles). Solid (blue) and broken (green) lines correspond to the Raman and fluorescence components, respectively. (b) Example of energy-dispersion for Raman and fluorescence components in the fitting for YMn_2 at 300 K.

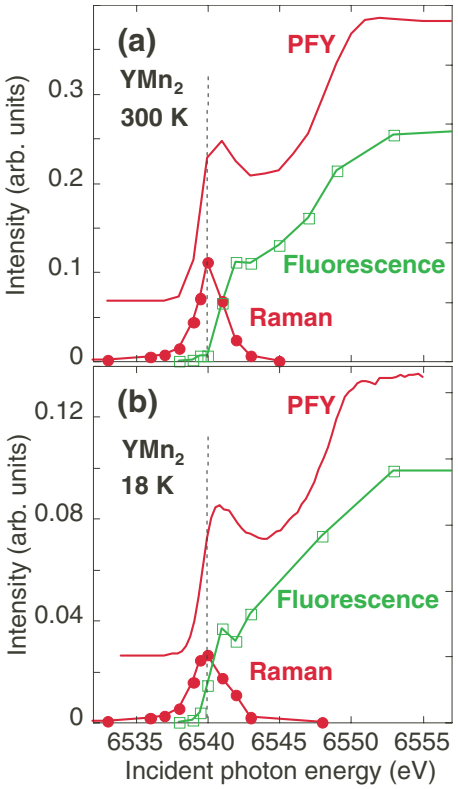

FIG. 6. (Color online) Results of the analysis of the RXES spectra of YMn_2, Raman (closed circle) and fluorescence (open square) components, at (a) 300 K and (b) 18 K.

The temperature dependence of the Mn $K\beta(3p \rightarrow 1s)$ emission measured by XES for both nonsubstituted and Lu-substituted samples is shown in Fig. 7. The intensities are normalized by the area under the curve. The exchange inter-

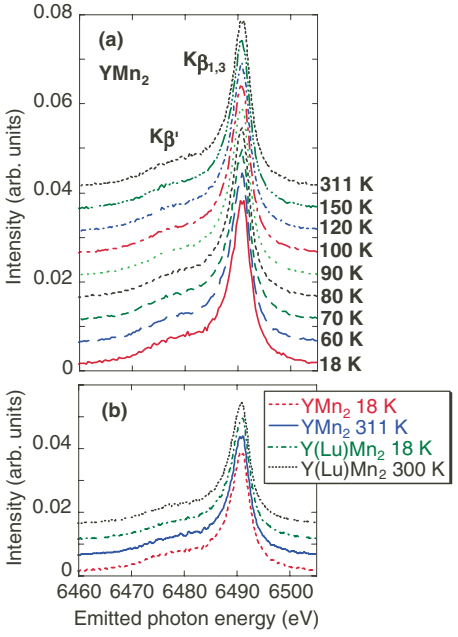

FIG. 7. (Color online) (a) Temperature dependence of the K_β emission spectrum obtained for YMn_2. (b) K_β emission spectra obtained for YMn_2 and $Y_{0.96}Lu_{0.04}Mn_2$ at 18 K and 300 K.

action between the $3p$ core hole and the $3d$ open shell in the final state splits the spectrum between the main line $K\beta_{1,3}$ and a low-energy satellite peak $K\beta'$, mostly corresponding to minority and majority of spins, respectively.[54–56] As seen in Fig. 7, no dependence on temperature or Lu substitution is observed. The intensity differences between the spectra are within experimental errors. Based on the value of the magnetic moment at low temperatures ($2.7\mu_B$) the Mn spin is estimated to be nearly $S=3/2$, thus in the high-spin (HS) state. From the absence of change in the line shape of the XES spectrum, we can conclude that the Mn sites retain their HS state despite the large volume expansion (5%) at the onset of the AF ordering around 100 K in YMn_2.

We studied the bulk electronic properties of Mn in YMn_2 and $Y_{0.96}Lu_{0.04}Mn_2$ using x-ray spectroscopies. Based on the data, we discussed the temperature and substitution dependence of the DOS near the Fermi edge and of the Mn spin state. YMn_2 and $Y_{0.96}Lu_{0.04}Mn_2$ show an opposite temperature dependence of their Mn-K pre-edge intensity, in line with their respective temperature-induced volume changes (low-temperature expansion for YMn_2 and contraction for $Y_{0.96}Lu_{0.04}Mn_2$) and the ensuing alteration of the hybridization strength. Relative delocalization of the Mn $3d$ states in YMn_2 is suggested by the $1s2p$ RXES data. No change in the Mn $K\beta$ line shape was found throughout 18–311 K in both compounds, indicating that the Mn spin remains in the high-spin state irrespective of the large volume change accompanying the onset of AF order.

The experiments were performed at BL15XU (under Proposal No. 07B19) of SPring-8, Japan Synchrotron Radiation Research Institute (JASRI). We thank H. Atsuta, D. Nomoto, and Y. Katsuya for the help in the experiment. Y. Nakamura and H. Akai are gratefully acknowledged for fruitful discussion.

[1] M. Shiga, Physica B **149**, 293 (1988).
[2] N. F. M. Henry and K. Lonsdale, *International Tables for X-ray Crystallography* (Kynoch, Birmingham, 1965), Vol. 1, p. 340.
[3] H. Wada, M. Shiga, and Y. Nakamura, Physica B **161**, 197 (1989).
[4] R. Ballou, J. Deportes, R. Lemaire, Y. Nakamura, and B. Ouladdiaf, J. Magn. Magn. Mater. **70**, 129 (1987).
[5] H. Nakamura, N. Metoki, S. Suzuki, F. Takayanagi, and M. Shiga, J. Phys.: Condens. Matter **13**, 475 (2001).
[6] J. Deportes, B. Ouladdiaf, and K. R. A. Ziebeck, J. Phys. (France) **48**, 1029 (1987).
[7] T. Freltoft, P. Böni, G. Shirane, and K. Motoya, Phys. Rev. B **37**, 3454 (1988).
[8] M. Shiga, H. Wada, Y. Nakamura, J. Deportes, B. Ouladdiaf, and K. R. A. Ziebeck, J. Phys. Soc. Jpn. **57**, 3141 (1988).
[9] K. Motoya, T. Freltoft, P. Böni, and G. Shirane, Phys. Rev. B **38**, 4796 (1988).
[10] R. Ballou, E. Leliévre-Berna, and B. Fåk, Phys. Rev. Lett. **76**, 2125 (1996).
[11] K. Yoshimura, M. Shiga, and Y. Nakamura, J. Phys. Soc. Jpn. **55**, 3585 (1986).
[12] C. Pinettes and C. Lacroix, J. Phys.: Condens. Matter **6**, 10093 (1994).
[13] M. Shiga, H. Wada, H. Nakamura, K. Yoshimrua, and Y. Nakamura, J. Phys. F: Met. Phys. **17**, 1781 (1987).
[14] S. Demuynck, S. N. Mishra, A. A. Tulapurkar, S. Cottenier, J. Meersschaut, and M. Rots, Physica B **293**, 376 (2001).
[15] M. R. Ibarra, L. Garcia-Orza, and A. del Moral, Solid State Commun. **84**, 875 (1992).
[16] J. Chaboy, A. Marcelli, M. R. Ibarra, and A. del Moral, Solid State Commun. **91**, 859 (1994).
[17] H. Nakamura, H. Wada, K. Yoshimura, M. Shiga, Y. Nakamura, J. Sakurai, and Y. Komura, J. Phys. F: Met. Phys. **18**, 981 (1988).
[18] S. Mondal, S. H. Kilcoyne, R. Cywinski, B. D. Rainford, and C. Ritter, J. Magn. Magn. Mater. **104-107**, 1421 (1992).
[19] J. Chaboy, C. Piquer, A. Marcelli, M. Battisti, G. Cibin, and L. Bozukov, Phys. Rev. B **58**, 77 (1998).
[20] I. S. Dubenko, I. Yu Gaidukova, Y. Hosokoshi, K. Inoue, and A. S. Markosyan, J. Phys.: Condens. Matter **11**, 2937 (1999).
[21] I. Yu. Gaĭdukova, I. S. Dubenko, R. Z. Levitin, A. S. Markosyan, and A. N. Pirogov, Sov. Phys. JETP **67**, 2522 (1988).
[22] R. Hauser, E. Bauer, E. Gratz, Th. Holubar, A. Indinger, A. Lindbaum, W. Perthold, I. S. Dunemko, and A. S. Markosyan, Physica B **206-207**, 17 (1995).
[23] G. Oomi, T. Terada, M. Shiga, and Y. Nakamura, J. Magn. Magn. Mater. **70**, 137 (1987).
[24] A. Block, M. M. Abd-Elmeguid, and H. Micklitz, Phys. Rev. B **49**, 12365 (1994).
[25] G.-Q. Zheng, K. Nishikido, K. Ohnishi, Y. Kitaoka, K. Asayama, and R. Hauser, Phys. Rev. B **59**, 13973 (1999).
[26] K. Kadowaki and S. B. Woods, Solid State Commun. **58**, 507 (1986).
[27] N. Tsujii, K. Yoshimura, and K. Kosuge, J. Phys.: Condens. Matter **15**, 1993 (2003); N. Tsujii, H. Kontani, and K. Yoshimura, Phys. Rev. Lett. **94**, 057201 (2005).
[28] K. Terao and M. Shimizu, Phys. Lett. **104A**, 113 (1984).
[29] H. Yamada and M. Shimizu, J. Phys. F: Met. Phys. **17**, 2249 (1987).
[30] A. Asano and S. Ishida, J. Phys. F: Met. Phys. **18**, 501 (1988).
[31] J. Kübler, L. M. Sandratskii, and M. Uhl, J. Magn. Magn. Mater. **104&107**, 695 (1992).
[32] Y. Nakamura and M. Shiga, Physica B **120**, 212 (1983).
[33] S. Iwasaki, T. Fukazawa, and H. Akai (unpublished): in the first principle calculations they use Korringa-Kohn-Rostoker Green's function method with coherent potential approximation. Further detail calculations are undergoing.
[34] K. Nakada, H. Shimizu, H. Yamada, and H. Harima, J. Magn. Magn. Mater. **262**, 374 (2003).
[35] J.-Y. Son, T. Mizokawa, A. Fujimori, K. Terao, H. Yamada, H. Wada, and M. Shiga, Solid State Commun. **127**, 237 (2003).
[36] H. Yamaoka, N. Tsujii, K. Yamamoto, H. Oohashi, A. M. Vlaicu, K. Kunitani, K. Uotani, D. Horiguchi, T. Tochio, Y. Ito, and S. Shin, Phys. Rev. B **76**, 075130 (2007).

[37] K. Yamamoto, H. Yamaoka, N. Tsujii, A. M. Vlaicu, H. Oohashi, S. Sakakura, T. Tochio, Y. Ito, A. Chainani, and S. Shin, J. Phys. Soc. Jpn. **76**, 124705 (2007).
[38] N. Tsujii, H. Yamaoka, H. Oohashi, I. Jarrige, D. Nomoto, K. Takahiro, K. Ozaki, and K. Kawatsura, Physica B **403**, 922 (2008).
[39] H. Yamaoka, H. Oohashi, I. Jarrige, T. Terashima, Y. Zou, H. Mizota, S. Sakakura, T. Tochio, Y. Ito, E. Ya. Sherman, and A. Kotani, Phys. Rev. B **77**, 045135 (2008).
[40] H. Yamaoka, N. Tsujii, H. Oohashi, D. Nomoto, I. Jarrige, K. Takahiro, K. Ozaki, K. Kawatsura, and Y. Takahashi, Phys. Rev. B **77**, 115201 (2008).
[41] A. Nisawa, M. Okui, N. Yagi, T. Mizutani, H. Yoshikawa, and S. Fukushima, Nucl. Instrum. Methods Phys. Res. A **497**, 563 (2003).
[42] D. Horiguchi, K. Yokoi, H. Mizota, S. Sakakura, H. Oohashi, Y. Ito, T. Tochio, A. M. Vlaicu, H. Yoshikawa, S. Fukushima, H. Yamaoka, and T. Shoji, Radiat. Phys. Chem. **75**, 1830 (2006).
[43] Q. Qian, T. A. Tyson, C.-C. Kao, M. Croft, S.-W. Cheong, G. Popov, and M. Greenblatt, Phys. Rev. B **64**, 024430 (2001).
[44] A. Bianconi, in *X-ray Absorption: Principles, Applications, Techniques of EXAFS, SEXAFS and XANES*, edited by D. C. Koningsberger and R. Prins (John Wiley & Sons, New York, 1988), Chap. 11 (and references therein).
[45] J. I. Espeso, J. C. Gómez Sal, and J. Chaboy, Phys. Rev. B **63**, 014416 (2000).
[46] J. Chaboy and C. Piquer, Phys. Rev. B **66**, 104433 (2002).
[47] M. Shiga and H. Wada, J. Magn. Magn. Mater. **151**, 225 (1995).
[48] M. Pajda, R. Ahuja, B. Johansson, J. M. Wills, H. Figiel, A. Paja, and O. Eriksson, J. Phys.: Condens. Matter **8**, 3373 (1996).
[49] T. Åberg and B. Crasemann, in *Resonant Anomalous X-ray Scattering Theory and Application*, edited by G. Materlik, C. J. Sparks, and K. Fischer (Elsevier Amsterdam, 1994), p. 431.
[50] I. Jarrige, H. Ishii, Y. Q. Cai, J.-P. Rueff, C. Bonnelle, T. Matsumura, and S. R. Shieh, Phys. Rev. B **72**, 075122 (2005).
[51] H. Yamaoka, M. Taguchi, A. M. Vlaicu, H. Oohashi, Y. Yokoi, D. Horiguchi, T. Tochio, Y. Ito, K. Kawatsura, K. Yamamoto, A. Chainani, S. Shin, M. Shiga, and H. Wada, J. Phys. Soc. Jpn. **75**, 034702 (2006).
[52] M. Deutsch, G. Hölzer, J. Härtwig, J. Wolf, M. Fritsch, and E. Förster, Phys. Rev. A **51**, 283 (1995).
[53] J.-P. Rueff, L. Journel, P.-E. Petit, and F. Farges, Phys. Rev. B **69**, 235107 (2004).
[54] K. Tsutsumi, J. Phys. Soc. Jpn. **14**, 1696 (1959).
[55] X. Wang, F. M. F. de Groot, and S. P. Cramer, Phys. Rev. B **56**, 4553 (1997).
[56] H. Yamaoka, M. Oura, M. Taguchi, T. Morikawa, K. Takahiro, A. Terai, K. Kawatsura, A. M. Vlaicu, Y. Ito, and T. Mukoyama, J. Phys. Soc. Jpn. **73**, 3182 (2004).